Nucleosomal arrangement affects single-molecule transcription dynamics

Veronika Fitz[a,b], Jaeoh Shin[c], Christoph Ehrlich[a,b], Lucas Farnung[d], Patrick Cramer[d], Vasily Zaburdaev[c], and Stephan W. Grill[a,b,c,1]

[a]Biotechnology Center, Technical University Dresden, 01307 Dresden, Germany; [b]Max Planck Institute of Molecular Cell Biology and Genetics, 01307 Dresden, Germany; [c]Max Planck Institute for the Physics of Complex Systems, 01187 Dresden, Germany; and [d]Department of Molecular Biology, Max Planck Institute for Biophysical Chemistry, 37077 Göttingen, Germany

Edited by Steven M. Block, Stanford University, Stanford, CA, and approved September 27, 2016 (received for review March 16, 2016)

In eukaryotes, gene expression depends on chromatin organization. However, how chromatin affects the transcription dynamics of individual RNA polymerases has remained elusive. Here, we use dual trap optical tweezers to study single yeast RNA polymerase II (Pol II) molecules transcribing along a DNA template with two nucleosomes. The slowdown and the changes in pausing behavior within the nucleosomal region allow us to determine a drift coefficient, χ, which characterizes the ability of the enzyme to recover from a nucleosomal backtrack. Notably, χ can be used to predict the probability to pass the first nucleosome. Importantly, the presence of a second nucleosome changes χ in a manner that depends on the spacing between the two nucleosomes, as well as on their rotational arrangement on the helical DNA molecule. Our results indicate that the ability of Pol II to pass the first nucleosome is increased when the next nucleosome is turned away from the first one to face the opposite side of the DNA template. These findings help to rationalize how chromatin arrangement affects Pol II transcription dynamics.

Pol II | transcription | single-molecule | optical tweezers | internucleosomal distance

To accommodate the massive amount of genetic material within the nucleus, DNA is packaged into chromatin. The level of chromatin compaction determines the accessibility of the underlying DNA, which in turn impacts gene expression (1). The first step in gene expression is transcription, where RNA polymerase II (Pol II) processively moves along the DNA template to generate an RNA copy. However, how chromatin impacts the translocation dynamics of individual RNA polymerases has remained unclear.

The fundamental unit of chromatin is a single nucleosome, which consists of 147 bp of DNA wrapped ∼1.7 times around a histone octamer (2). In vitro experiments have revealed that a single nucleosome exhibits a significant mechanical barrier to the transcribing Pol II (3–7). Using optical tweezers, it was shown that a nucleosome both decreases the rate of forward translocation and increases polymerase pausing and backtracking (3, 5). These changes have been suggested to depend on the unwrapping dynamics of the nucleosome itself, which are governed by nucleosomal properties such as the histones' modification state as well as the underlying DNA sequence (3, 5).

In vivo, the process of chromatin transcription is far more complex. Chromatin accessibility is affected by many accessory factors that facilitate the progression of RNA polymerases through nucleosomal obstacles (1). A central outstanding question is to what extent the nucleosomal arrangement affects Pol II transcription behavior. This arrangement might be particularly important in budding yeast, an organism with a compact genome with short internucleosomal distances (8–11).

Here, we study the impact of the arrangement of two nucleosomes on the nucleosomal transcription performance of individual molecules of Pol II. We use dual-trap optical tweezers in a single-molecule approach to follow single enzymes of Pol II as they progress through a dinucleosomal array (3, 5). Specifically we investigate how Pol II passage through the first nucleosome depends on the length of the linker DNA between the two nucleosomes.

Results

Single-Molecule Transcription Through a Single Nucleosome. We first sought to recapitulate single-molecule results obtained from Pol II transcription experiments along mononucleosomal templates (3, 5). We expressed and purified the four canonical yeast histones from *Escherichia coli* without posttranslational modifications. After refolding the histone octamers, we assembled the yeast nucleosomes on the artificial Widom601 nucleosome positioning sequence (NPS) (12), which exhibits a high affinity for the histone octamer. Protocols were adapted from refs. 13 and 14 (*SI Text*). The use of the strong nucleosome positioning sequence, the Widom601, ensures exact positioning of the nucleosomes, which is crucial for our experiments as we analyze changes in transcription dynamics within this well-defined region. We determined the quality of all nucleosomal reconstitutions by both a gel-based assay (*SI Text* and Fig. S1*A*) and force–extension measurements (*SI Text* and Fig. S1*B*). Pol II was purified from yeast as described in ref. 15. We assembled transcription elongation complexes as described in refs. 15 and 16 and subsequently ligated them in a single ligation reaction to both the naked upstream DNA and the downstream DNA template with already assembled nucleosome(s) (*SI Text* and Fig. S2 shows all nucleosomal templates used in this study). In the dual-trap optical tweezers, we formed a tether between two polystyrene beads: one attached to the polymerase and the other to the upstream DNA (*SI Text* and Fig. 1*A*). On buffer exchange and addition

Significance

Transcription is the first step toward protein production. During transcription, a polymerase enzyme moves along DNA and copies it to RNA. In the cell, DNA is highly compacted: roughly 150 bp of DNA is wrapped around histone proteins to form a nucleosome. However, little is known about how closely spaced nucleosomes impact polymerase transcription. We performed single-molecule optical tweezers transcription experiments on dinucleosomal DNA templates. We show that the effect of the second nucleosome on polymerase transcription efficiency through the first one depends on the internucleosomal spacing and the rotational arrangement of the nucleosomes on the helical DNA template. Our findings provide insights into how DNA compaction affects transcription in vitro.

Author contributions: V.F., P.C., V.Z., and S.W.G. designed research; V.F., J.S., and L.F. performed research; V.F., C.E., and L.F. contributed new reagents/analytic tools; V.F. and J.S. analyzed data; and V.F., J.S., P.C., V.Z., and S.W.G. wrote the paper.

The authors declare no conflict of interest.

This article is a PNAS Direct Submission.

Freely available online through the PNAS open access option.

[1]To whom correspondence should be addressed. Email: stephan.grill@biotec.tu-dresden.de.

This article contains supporting information online at www.pnas.org/lookup/suppl/doi:10.1073/pnas.1602764113/-/DCSupplemental.

of ribonucleotide triphosphates (NTP), Pol II began to translocate along the DNA toward the nucleosome (*SI Text* and Fig. 1*A*). Note that the nucleosome was not under tension from the optical traps, because it is positioned downstream (Fig. 1*A*). Experiments were done under assisting force (typically 9 ± 1 pN when encountering the nucleosome; *SI Text*). Experiments were performed in the presence of 60 mM $(NH_4)_2$ SO_4, which corresponds to an ionic strength of ~120 mM. The region of nucleosomal influence (200 bp) was defined according to Bintu et al. (3) (Fig. 1*B*).

In agreement with previous work (3, 5), we found that the transcription behavior of Pol II changes significantly in the presence of a nucleosome (Fig. 1*C*). Dwell times (the average time the polymerase resides at a base pair) were increased at the nucleosome, in particular within its central part. This part of the nucleosomal DNA corresponds to the dyad region, which is known to be difficult to pass for a polymerase (3, 5) (Fig. 1*D*). This increase in dwell times comes about because the Pol II elongation rate decreases, whereas pause frequency and pause duration increase (Table S1 and Fig. 1*E*). Furthermore, we find that it takes individual Pol II molecules 63.5 ± 15.5 s (mean ± SEM unless otherwise noted) to pass a single nucleosome (Table S1). This time, which we refer to as residence time, is approximately five times longer than the average value measured at the same location but without a nucleosome (Fig. 1*F*). Importantly, detecting this increase in residence time also allows us to test in each experiment for the presence of the first nucleosome (*SI Text* and Fig. S3*A*). We operationally define a single Pol II molecule as unable to efficiently pass the nucleosome when it remains for more than 145 s within the nucleosomal region (66.04 + 2 × 39.68 s, mean + 2 SDs of the nucleosomal residence time of all polymerases that make it through the nucleosomal region; for polymerases that did not pass the first nucleosomal region, only those traces with passage times longer than the cutoff time of 145 s were considered; *SI Text* and Fig. S3*B*). With this definition, 8% of all measured Pol II molecules are unable to efficiently pass the single nucleosome (Fig. 1*G*). To conclude, in agreement with earlier work (3, 5), we find that, although single molecules of Pol II slow down significantly when they encounter a nucleosome, a large majority successfully makes it through.

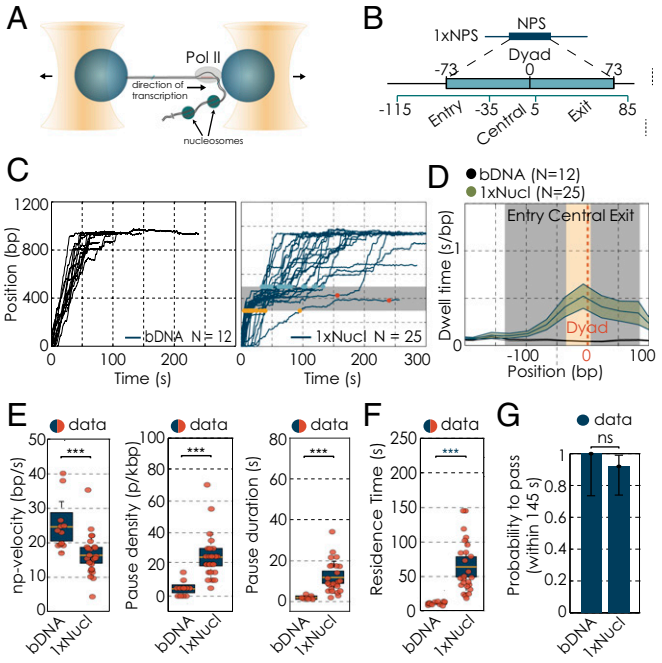

Fig. 1. Single-molecule transcription elongation by RNA polymerases II through single nucleosome. (*A*) Dual-trap optical tweezers, assisting force arrangement. (*B*) Region of nucleosomal influence according to Bintu et al. (3). (*C*) Transcription traces of individual Pol II molecules, transcribing along a single nucleosomal templates where no nucleosome has been present, bare DNA (bDNA; *Left*) or a nucleosome was present (1xNucl; *Right*) (data filtered at 1-kHz bandwidth). The gray bar illustrates the position of the nucleosome. Yellow and blue dots highlight the position at which polymerases enter and exit the nucleosome, respectively. For polymerases that did not transcribe through the nucleosomal region within 145 s, red dots mark their position at 145 s after entering the nucleosomal region. (*D*) Changes in dwell time distributions along mononucleosomal DNA template, zoomed into the nucleosomal region. The gray bar illustrates the position of the nucleosome; the yellow area marks the central region. Dwell time distributions for the mononucleosomal DNA template in the absence of a nucleosome (black) and in the presence of a nucleosome (green). The solid line represents the mean, whereas the shaded areas show the respective SEM. (*E*) Changes in transcription parameters on mononucleosomal DNA template with and without a nucleosome: changes in pause-free velocities (*Left*). Pause densities (*Center*) and pause durations (*Right*). Quantifications for each transcription parameters are shown as box plots, where the central mark is the mean, the edges of the box are the SEM and the whiskers are the SDs. The red dots represent values for single experiments. (*F*) Residence times for transcription on mononucleosomal DNA template. (*G*) Quantification of the passage probabilities through the single nucleosomal region. The passage probability refers to the capacity of a polymerase to pass the nucleosomal region within the cutoff time of 145 s. The error bars represent 95% CI. Experimental data are shown in blue; theory is shown in green. We used the Barnard's exact test to calculate the *P* values for binary data sets. *N* indicates the number of Pol II transcription trajectories on each template. Two datasets are considered significantly different if the *P* value is below or equal to 0.05. Different *P* values are indicated as follows: ns, $P > 0.05$; ***$P \leq 0.001$.

We also observe that most of the Pol II molecules do not return to "normal" transcription behavior after passing the nucleosomal region, but instead appear to pause more frequently than they do on naked DNA (Fig. 1*C*). This behavior was reported before (at 150 mM salt, comparable to 120 mM used here) (5), but interpreting postpassage pausing is difficult as the measurement of position in the optical tweezers is no longer calibrated (*SI Text*). It is interesting to speculate that a nucleosome that was passed might remain in contact with Pol II and affect its postpassage pausing behavior. Here, we only analyze changes in transcription dynamics within the nucleosomal region and not beyond.

Although Pol II molecules reduced their elongation rate within the nucleosomal region, we speculated that it was their inability to recover from long pauses which rendered them unable to pass the barrier (within 145 s). Specifically, we speculated that the decreased elongation rate at the nucleosome and the decreased passage probability are quantitatively related. In particular, we wondered if it is possible to predict Pol II nucleosomal passage probabilities from the measured reduction in elongation rate and the increase in the number of pauses within the nucleosomal region, compared with transcription on naked DNA. For this, we extend a stochastic description of transcription dynamics (5), combining the idea that the nucleosome acts as a fluctuating barrier (5) with the biased diffusion model for backtracking (17) to investigate Pol II transcription dynamics on different nucleosomal templates.

A Stochastic Model of Transcription Elongation. We assume that during active transcription on bare DNA, Pol II elongates with rate k_e (Fig. 2*A*). This rate is known to be dependent on the force F applied in the optical tweezers (18, 19). However, due to the narrow range of entry forces and the small decrease of the force over the nucleosomal region in our experiments, we expect the applied force to change the elongation rate k_e by less than 5% (*SI Text*). Therefore, in what follows, we consider k_e to be independent of the applied force. At each template position Pol II can enter a backtrack, which results in the displacement of the RNA 3′ end from the active site and renders Pol II transcriptionally inactive. In the backtracked state, the enzyme can passively diffuse along the DNA with the forward and backtracking rates k_f

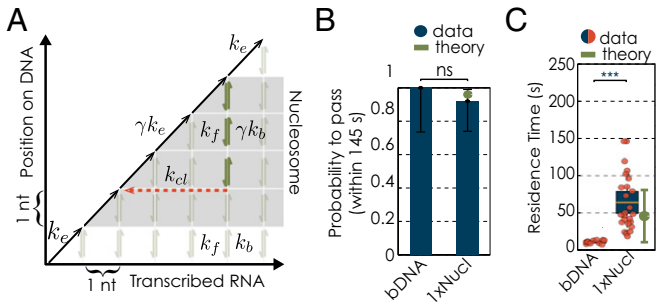

Fig. 2. Stochastic model of transcription elongation in presence of a nucleosome: (*A*) Illustration of stochastic model: The *x* axis represents the transcribed RNA, and the *y* axis the position of Pol II along the DNA template. On bare DNA, the polymerase moves in the diagonal direction with the elongation rate k_e. In the transcriptionally inactive state, the polymerase diffuses forward and backward in the vertical direction with the rates k_f and k_b, respectively. Cleavage of the displaced RNA transcript with the rate k_{cl} results in a horizontal move. The gray region indicates the position of the nucleosome. In the presence of a nucleosome both the elongation rate k_e and the forward hopping rate k_f decrease by the factor γ. (*B*) Quantification of the passage probabilities through the single nucleosomal region in presence or absence of nucleosome. The passage probability refers to the capacity of a polymerase to pass the nucleosomal region within the cutoff time of 145 s. The error bars represent 95% CI. Experimental data are shown in blue; theory is shown in green. We used the Barnard's exact test to calculate the *P* values for binary datasets. Numbers of trajectories per condition as in Fig. 1. Two data sets are considered significantly different if the *P* value is below or equal to 0.05. Different *P* values are indicated as follows: ns, $P > 0.05$; ***$P \leq 0.001$. (*C*) Residence times for all conditions (data in red/blue and theory in green).

and k_b, respectively (Fig. 2*A*). Both the forward and backtrac-king rates are influenced by the applied force F according to $k_f = k_0 \exp[+Fa/(k_B T)]$ and $k_b = k_0 \exp[-Fa/(k_B T)]$, where k_0 denotes the intrinsic hopping rate in the absence of force (17, 19–21), a is the distance to the transition state, and $k_B T$ is the thermal energy. We assume a to be 0.17 nm (5, 17), which places the transition state symmetrically between two base pair positions (spaced 0.34 nm apart). The exit from the backtracked state proceeds in a competition between two processes (22): first, realignment of the RNA 3′ end with the active site when Pol II returns to the starting point of its backtrack by passive diffusion; and second, intrinsic cleavage of the RNA 3′ overhang with rate $k_{cl} = 0.012 \pm 0.003\ s^{-1}$ (22). Importantly, both processes lead to a reinitiation of active transcription.

To account for the presence of the nucleosomal barrier, the Bustamante laboratory has shown that local transient unwrapping of the DNA from the histone octamer allows the polymerase to pass further into the nucleosome (5). Following Hodges et al., we use γ to denote the fraction of time the downstream DNA is locally unwrapped from the histone octamer (5). Because the polymerase can only step further when the DNA is accessible (unwrapped), both k_f and k_e are decreased by the factor γ within the nucleosomal region (5) (see shaded region in Fig. 2*A*). The DNA upstream of Pol II is under mechanical tension, and we assume that the DNA remains unwrapped from the nucleosome once the polymerase has passed through it (5). Therefore, the nucleosomal backtracking rate k_b remains unchanged from the value on bare DNA.

Importantly, the parameter γ can be directly obtained from the experimental data as the ratio of pause-free velocities (v_e) within the nucleosomal region and pause-free velocities within the same region of the same DNA template but without a nucleosome

$$\gamma = v_e(\text{nucleosome})/v_e(\text{bare}). \quad [1]$$

From our experiments, we find that γ assumes a value of 0.67 ± 0.11 in the presence of a single nucleosome.

We define the pause density P_{pause} as the number of pauses per kilobase pair, which can be expressed as

$$P_{pause} = \frac{k_b}{k_b + \gamma k_e} = \frac{k_0 \exp[-Fa/(k_B T)]}{k_0 \exp[-Fa/(k_B T)] + \gamma k_e}. \quad [2]$$

From our experimental data, we determine k_0 to be 0.56 ± 0.14 s^{-1}, which is in general agreement with earlier results (22) (Table S2).

Within this model, the ability of Pol II to transcribe through the nucleosome sensitively depends on the effectiveness of the enzyme to recover from a nucleosomal backtrack. The ability to recover from a backtrack, however, depends on whether during backtracking the polymerase is more likely to step further into a backtrack or step in the direction out of the backtrack. If at every nucleosomal backtrack position it is more likely for the polymerase to step further into a backtrack than out, nucleosomal backtracking pauses will be of long duration and the chance of arrest within the nucleosome will be large. The ratio χ between forward and backward hopping rates in the nucleosomal region is given by

$$\chi = k_f/k_b = \gamma \exp[2Fa/(k_B T)]. \quad [3]$$

This dimensionless "drift coefficient" χ defines two regimes of Pol II nucleosomal transcription dynamics. If χ is larger than 1, Pol II can easily recover and resume active elongation. Conversely for $\chi < 1$, Pol II is more likely to step deeper into the backtrack. The increased likelihood to step deeper into a backtrack results in longer pauses and even arrest, because backtrack recovery can no longer occur via diffusion but through slow intrinsic transcript cleavage (with a time constant of $k_{cl}^{-1} \sim 80$ s) (22). Hence the value of χ determines whether Pol II manages to pass the nucleosome or is likely to get trapped within the nucleosomal region. Because ∼92% of the polymerases are able to pass the single nucleosome (Fig. 1*G*), we expect χ to be larger than 1. Consistent with this expectation, we find that χ is equal to 1.35 ± 0.25 for the single nucleosome condition (Table S2). We conclude that the drift coefficient χ quantifies the impact of the nucleosome on Pol II transcription dynamics.

To summarize, the quantities we used in the model were the entry force when Pol II arrives to the nucleosomal DNA, decrease of the pause-free velocity in the nucleosomal region, and the pause density. Although the first two parameters determine the χ parameter, all three of them are related to the elongation of Pol II. The two important quantities that can be calculated with the help of the model are residence time and the passage probability. Importantly, those are determined by both the elongation and the backtracking dynamics together. Our model, however, provides information on the backtracking dynamics from the measurements of the elongation dynamics. In this respect, the results on the passage probability given by the model can be considered as a prediction, based on the empirically determined elongation parameters.

To test whether we are able to predict Pol II nucleosomal passage probabilities from the measured value of χ, we generated ∼10^5 Pol II transcription trajectories via kinetic Monte Carlo simulations (23) using the calculated value of χ (*SI Text*). We find that both passage probabilities and residence times (within 145 s) through the nucleosome obtained from numerical simulations are consistent within errors with those measured in experiments (Fig. 2 *B* and *C*). Note that calculated residence times show a broad distribution, owing to the stochasticity of the transcription process. Thus, we are able to predict Pol II nucleosomal passage probabilities from the measured reduction in elongation rate and the increase in the number of pauses within the nucleosomal region as captured by χ. Next, we use this theoretical analysis to

quantify which properties of nucleosomal transcription are affected on addition of a second nucleosome.

The Presence of a Second Nucleosome Impairs Pol II Transcription Dynamics Through the First Nucleosome by Reducing the Drift Coefficient χ. To test whether the presence of a second nucleosome affects Pol II transcription dynamics through the first nucleosome, we investigated transcription dynamics of individual Pol II enzymes along dinucleosomal templates. We performed our initial experiments on dinucleosomal templates with an internucleosomal spacing of 50 bp, which is larger than the typical spacing in yeast (23 bp) (8) but smaller than the typical spacing in higher eukaryotes (60 bp) (24).

Strikingly, we find that placing a second nucleosome 50 bp downstream of the first one considerably affects Pol II transcription dynamics within the first nucleosome (Fig. 3*A*): dwell times are highly increased within the central region of the first nucleosome compared with the mononucleosomal condition (Fig. 3*B*). Nucleosomal residence times increased almost twofold to 118.9 ± 23.0 s (Fig. 3*C*) due to a decreased elongation rate and an increase of both pause frequency and duration (Fig. 3*D*). Importantly, the passage probability decreased to ∼28% (Fig. 4 *A* and *B*). Note that, although we used Pol II slowdown dynamics in the first nucleosomal region to detect the presence of the first nucleosome, we cannot perform a similar analysis to detect the presence of the second nucleosome (*SI Text*). Given that we expect the second nucleosome to actually be absent in a small fraction of experiments (Fig. S1*B*), we thus slightly underestimate the impact of the second nucleosome on the transcription dynamics through the first.

In the framework of our stochastic model, we expect that this significant reduction in passage probabilities is caused by the factor χ dropping below 1. Indeed, pause densities are increased more than sevenfold and γ drops to 0.48 ± 0.12, resulting in the drift coefficient χ to be reduced to 0.87 ± 0.22 (Tables S1 and S2 and Fig. 3*D*). Similar to the single nucleosome condition, we are capable with this measured value of χ to recapitulate within errors the residence time within and to predict passage probability through the first nucleosome (Figs. 3*C* and 4*B*). To conclude, the ability of Pol II to progress through a nucleosome is severely impeded by placing a second nucleosome 50 bp downstream. The second nucleosome reduces the drift coefficient χ to a value below 1, rendering Pol II ineffective in rapidly recovering from backtracks within the first nucleosome.

The Internucleosomal Arrangement Affects Pol II Transcription Dynamics. We next sought to investigate whether the impact of the second nucleosome on Pol II transcription dynamics through the first one depends on internucleosomal spacing. We therefore studied dinucleosomal compounds with different spacings. A linker length of 99 bp corresponds to ∼34 nm, which is approximately three times larger than the diameter of the single nucleosome (∼11 nm). We thus expect that at this internucleosomal distance, the impact of the second nucleosome on the transcription dynamics through the first one is reduced. Indeed, we observed that increasing the distance between the two nucleosomes to 99 bp resulted in an essentially complete recovery of Pol II transcription dynamics through the first nucleosome, which were now indistinguishable from Pol II dynamics in the presence of a single nucleosome only (Figs. 1*C* and 3 *A*–*D*). Furthermore, the calculated value of χ is 1.46 ± 0.30, and thus the passage probability reached ∼92%, again both similar to the single nucleosome condition (Fig. 4*B* and Table S2). This result suggests that the presence of a second nucleosome per se does not impact the transcription dynamics through the first. Instead, this impact only arises when the two neighboring nucleosomes are sufficiently close.

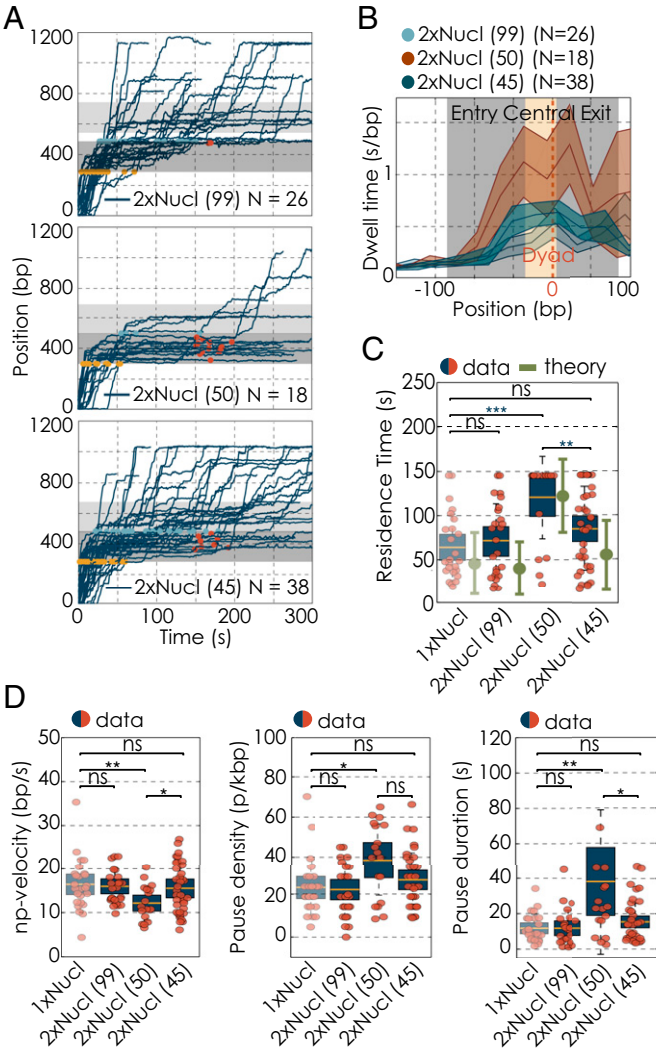

Fig. 3. Single-molecule transcription elongation by RNA polymerases II along dinucleosomal DNA templates. (*A*) Transcription traces of individual Pol II molecules, transcribing along a different dinucleosomal DNA templates: 99-bp linker (*Top*), 50-bp linker (*Middle*), and 45-bp linker (*Bottom*) (data filtered at 1-kHz bandwidth). The gray bar illustrates the position of the nucleosome. Yellow and blue dots highlight the position at which polymerases enter and exit the nucleosome, respectively. For polymerases that did not transcribe through the nucleosomal region within 145 s, red dots mark their position at 145 s after entering the nucleosomal region. (*B*) Changes in dwell time distributions along different dinucleosomal DNA templates, zoomed into the first nucleosomal region. The gray bar illustrates the position of the nucleosome; the yellow area marks the central region. Dwell time distribution for the 99-bp linker template (light blue), 50-bp linker (red), and 45-bp linker template (dark blue). The solid line represents the mean, whereas the shaded areas show the respective SEM. (*C*) Residence times for transcription on dinucleosomal DNA template (data in red/blue and theory in green). (*D*) Changes in transcription parameters on different dinucleosomal DNA templates with and without a nucleosome: changes in pause-free velocities (*Left*). Pause densities (*Center*) and pause durations (*Right*). Quantifications for each transcription parameter are shown as box plots, where the central mark is the mean, the edges of the box are the SEM, and the whiskers are the SDs. The red dots represent values for single experiments. *N* indicates the number of Pol II transcription trajectories on each template. Two datasets are considered significantly different if the *P* value is below or equal to 0.05. Different *P* values are indicated as follows: ns, $P > 0.05$; *$P \leq 0.05$; **$P \leq 0.01$; and ***$P \leq 0.001$.

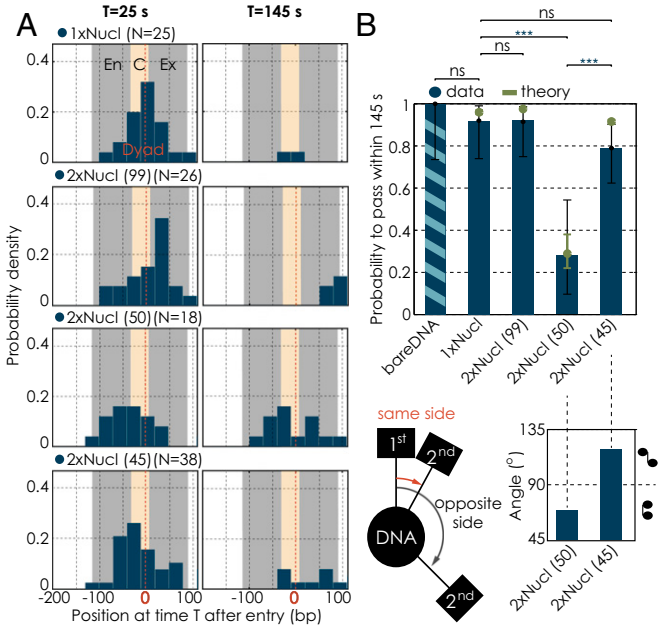

Fig. 4. Change in passage probabilities in the presence of a second nucleosome as a function of internucleosomal distance. (*A*) Residence distributions of polymerases at 25 s (*Left*) and 145 s (*Right*) after entering the first nucleosomal region for the different conditions. Note that some enzymes are outside of the field of view. The gray bar illustrates the position of the nucleosome (En, entry; Ex, exit); the yellow area marks the central region (C, central). (*B*) Quantification of the passage probabilities through the first nucleosomal region. The passage probability refers to the capacity of a polymerase to pass the nucleosomal region within the cutoff time of 145 s. Note that our results are not sensitive to the precise value of the cutoff chosen to define passage probabilities (Fig. S4) nor is there a dependency on force for the range of forces applied (Fig. S5). Error bars represent the 95% CI. Experimental data are shown in blue; theory is shown in green. We used the Barnard's exact test to calculate the *P* values for binary data sets. (*C*) (*Left*) Differences in nucleosomal orientations, where the two neighboring nucleosomes lie on the same or on opposite sides of the DNA. (*Right*) Angular distributions of the two neighboring nucleosomes for the 50- and 45-bp linker templates. Numbers of trajectories per condition as in Fig. 3. Two datasets are considered significantly different if the *P* value is below or equal to 0.05. Different *P* values are indicated as follows: ns, $P > 0.05$; ***$P \leq 0.001$.

Given the helical nature of the DNA molecule, we hypothesize that not only the distance in base pairs but also the rotational arrangement of the two nucleosomes with respect to each other impact the transcription dynamics through the first nucleosome (Fig. 4*C*, *Left*). We thus tested whether changing the rotational arrangement between the two neighboring nucleosomes affects the drift coefficient χ and the Pol II transcription performance through the first nucleosome. With the 50-bp internucleosomal spacing, the two nucleosomes face the same side of the DNA helix (Fig. 4*C*). Given that 10.4 bp corresponds to one full DNA helical turn, decreasing the spacing by 5 bp (i.e., half a helical turn) brings the two nucleosomes closer together in terms of base pair distance, but now places them toward opposite sides of the DNA and hence further apart overall (8, 25, 26) (Fig. 4*C*). Strikingly, we find that for the 45-bp linker, nucleosomal residence times are significantly decreased, and passage probabilities are greatly increased compared with the 50-bp linker condition (Tables S1 and S2 and Figs. 3*C* and 4*B*). Hence, reducing the internucleosomal distance from 50 to 45 bp greatly reduces the impact of the second nucleosome on the transcription dynamics through the first one. Consistent with this observation, we determine χ to be 1.29 ± 0.30 for a spacing of 45 bp. This value is above 1; hence, Pol II is able to rapidly recover from backtracks. Consequently, ~79% of all single RNA polymerases tested on the template with an internucleosomal spacing of 45 bp are able to exit the first nucleosomal region (within 145 s) (Fig. 4 *A* and *B* and Fig. S6), in good agreement with the value predicted from theory (Fig. 4*B*). Although more experiments with a broader range of linker lengths are necessary to demonstrate a helical phasing effect, we conclude that Pol II transcription dynamics and passage probabilities through the first nucleosome depend on the length of the linker DNA and on the rotational offset between the two neighboring nucleosomes.

Discussion

Here, we performed single-molecule transcription experiments along dinucleosomal templates differing in their internucleosomal arrangement. We discover that a second nucleosome affects Pol II nucleosomal transcription dynamics through the first nucleosome (as quantified by the drift coefficient χ) and the ability to pass it, whereby a decreased distance in base pairs between the two neighboring nucleosomes can be compensated by the rotational offset between them. Placing the two nucleosomes on opposite sides of the DNA helix results in Pol II nucleosomal transcription dynamics similar to what is obtained without the second nucleosome. Hence, the internucleosomal arrangement between the two neighboring nucleosomes impacts the transcription dynamics through the first nucleosome. However, how is this effect realized? How can the second nucleosome influence the transcription dynamics through the first one? One possibility is that the stability of the first nucleosome on the DNA templates is affected by the presence of the second nucleosome. We tested for such an effect by performing force–extension measurements, to determine nucleosome–DNA stability by measuring at which forces nucleosomes unwrap from DNA. However, we found that nucleosomal stabilities were similar for all of the different dinucleosomal templates (*SI Text*, Fig. S7, and Table S3). Thus, we conclude that the observed differences in transcription dynamics cannot be attributed to differences in nucleosomal stabilities for the different dinucleosomal templates. This result suggests that the transcribing Pol II enzyme itself mediates this intercommunication between the two neighboring nucleosomes and the corresponding changes in the transcriptional drift coefficient χ we have measured. A molecular model (Fig. S8), where we positioned the elongating Pol II complex in the exit region (past the dyad) of the first nucleosome, lends credence to this interpretation. The model shows that in the context of an elongating polymerase, internucleosomal distances differ for the two geometries. Contacts between the two neighboring nucleosomes are more likely with the 50-bp linker compared with the 45-bp linker (45-bp linker with ~130 Å vs. 50-bp linker with ~110 Å; Fig. S8). However, further studies are required to identify the molecular basis of how the second nucleosome influences transcription through the first. Interestingly, in vivo histones are highly modified and known to affect Pol II transcription efficiencies through nucleosomes. An interesting line of future research is to understand to what extent histone modifications modulate this geometry and the impact on the transcribing Pol II enzyme.

Finally, we note that earlier work has shown that yeast exhibits a very tight nucleosomal organization, with adjacent nucleosomes placed on opposite sides of the DNA helix due to the offset of one-half a helical turn (8–11). Our results therefore suggest that this type of nucleosomal arrangement might be critical for efficient chromatin transcription by RNA polymerase II.

ACKNOWLEDGMENTS. We thank M. Jahnel for building and maintaining the optical tweezers instrument; A. Lisica, S. Stoynov, and M. Nishikawa for fruitful discussions and suggestions; S. Sainsbury for providing Pol II; and N. Luzzietti and R. Seidel for providing the NPS. P.C. was supported by Deutsche Forschungsgemeinschaft (DFG) Grants SFB646, SFB960, SFB1064, GRK1721, CIPSM, NIM, and QBM; the Advanced Investigator Grant TRANSIT

of the European Research Council; and the Volkswagen Foundation. S.W.G. was supported by the DFG (Grants SPP 1782, GSC 97, GR 3271/2, GR 3271/3, and GR 3271/4), European Research Council Grant 281903, Innovative Training Networks (ITN) Grants 281903 and 641639 from the European Union, the Max Planck Society as a Max Planck Fellow, and Human Frontier Science Program Grant RGP0023/2014.

1. Elgin SC, Workman JL (2000) *Chromatin Structure and Gene Expression* (Oxford Univ Press, Oxford, UK), Vol 35.
2. Luger K, Mäder AW, Richmond RK, Sargent DF, Richmond TJ (1997) Crystal structure of the nucleosome core particle at 2.8 A resolution. *Nature* 389(6648):251–260.
3. Bintu L, et al. (2012) Nucleosomal elements that control the topography of the barrier to transcription. *Cell* 151(4):738–749.
4. Bondarenko VA, et al. (2006) Nucleosomes can form a polar barrier to transcript elongation by RNA polymerase II. *Mol Cell* 24(3):469–479.
5. Hodges C, Bintu L, Lubkowska L, Kashlev M, Bustamante C (2009) Nucleosomal fluctuations govern the transcription dynamics of RNA polymerase II. *Science* 325(5940): 626–628.
6. Izban MG, Luse DS (1991) Transcription on nucleosomal templates by RNA polymerase II in vitro: Inhibition of elongation with enhancement of sequence-specific pausing. *Genes Dev* 5(4):683–696.
7. Kireeva ML, et al. (2002) Nucleosome remodeling induced by RNA polymerase II: Loss of the H2A/H2B dimer during transcription. *Mol Cell* 9(3):541–552.
8. Brogaard K, Xi L, Wang JP, Widom J (2012) A map of nucleosome positions in yeast at base-pair resolution. *Nature* 486(7404):496–501.
9. Lohr D, Van Holde KE (1979) Organization of spacer DNA in chromatin. *Proc Natl Acad Sci USA* 76(12):6326–6330.
10. Lohr D (1986) The salt dependence of chicken and yeast chromatin structure. Effects on internucleosomal organization and relation to active chromatin. *J Biol Chem* 261(21):9904–9914.
11. Wang JP, et al. (2008) Preferentially quantized linker DNA lengths in Saccharomyces cerevisiae. *PLOS Comput Biol* 4(9):e1000175.
12. Lowary PT, Widom J (1998) New DNA sequence rules for high affinity binding to histone octamer and sequence-directed nucleosome positioning. *J Mol Biol* 276(1): 19–42.
13. Dyer PN, et al. (2004) Reconstitution of nucleosome core particles from recombinant histones and DNA. *Methods Enzymol* 375:23–44.
14. Luger K, Rechsteiner TJ, Richmond TJ (1999) Expression and purification of recombinant histones and nucleosome reconstitution. *Methods Mol Biol* 119:1–16.
15. Sydow JF, et al. (2009) Structural basis of transcription: Mismatch-specific fidelity mechanisms and paused RNA polymerase II with frayed RNA. *Mol Cell* 34(6):710–721.
16. Komissarova N, Kireeva ML, Becker J, Sidorenkov I, Kashlev M (2003) Engineering of elongation complexes of bacterial and yeast RNA polymerases. *Methods Enzymol* 371: 233–251.
17. Depken M, Galburt EA, Grill SW (2009) The origin of short transcriptional pauses. *Biophys J* 96(6):2189–2193.
18. Larson MH, et al. (2012) Trigger loop dynamics mediate the balance between the transcriptional fidelity and speed of RNA polymerase II. *Proc Natl Acad Sci USA* 109(17):6555–6560.
19. Dangkulwanich M, et al. (2013) Complete dissection of transcription elongation reveals slow translocation of RNA polymerase II in a linear ratchet mechanism. *eLife* 2:e00971.
20. Galburt EA, et al. (2007) Backtracking determines the force sensitivity of RNAP II in a factor-dependent manner. *Nature* 446(7137):820–823.
21. Ishibashi T, et al. (2014) Transcription factors IIS and IIF enhance transcription efficiency by differentially modifying RNA polymerase pausing dynamics. *Proc Natl Acad Sci USA* 111(9):3419–3424.
22. Lisica A, et al. (2016) Mechanisms of backtrack recovery by RNA polymerases I and II. *Proc Natl Acad Sci USA* 113(11):2946–2951.
23. Kafri Y, Nelson DR (2005) Sequence heterogeneity and the dynamics of molecular motors. *J Phys Condens Matter* 17(47):S3871–S3886.
24. Van Holde KE (2012) *Chromatin* (Springer Science & Business Media, New York).
25. Levitt M (1978) How many base-pairs per turn does DNA have in solution and in chromatin? Some theoretical calculations. *Proc Natl Acad Sci USA* 75(2):640–644.
26. Wang JC (1979) Helical repeat of DNA in solution. *Proc Natl Acad Sci USA* 76(1): 200–203.
27. Kireeva ML, Lubkowska L, Komissarova N, Kashlev M (2003) Assays and affinity purification of biotinylated and nonbiotinylated forms of double-tagged core RNA polymerase II from Saccharomyces cerevisiae. *Methods Enzymol* 370:138–155.
28. Galburt EA, Grill SW, Bustamante C (2009) Single molecule transcription elongation. *Methods* 48(4):323–332.
29. Selvin PR, et al. (2008). In vitro and in vivo FIONA and other acronyms for watching molecular motors walk. *Single-Molecule Techniques: A Laboratory Manual*, eds Selvin PR , Ha T (Cold Spring Harbor Press, Cold Spring Harbor, NY), pp 37–71.
30. Mack AH, et al. (2013) The molecular yo-yo method: Live jump detection improves throughput of single-molecule force spectroscopy for out-of-equilibrium transitions. *Rev Sci Instrum* 84(8):085119.
31. Mihardja S, Spakowitz AJ, Zhang Y, Bustamante C (2006) Effect of force on mononucleosomal dynamics. *Proc Natl Acad Sci USA* 103(43):15871–15876.
32. Marko JF, Siggia ED (1995) Stretching DNA. *Macromolecules* 28(26):8759–8770.
33. Adelman K, et al. (2002) Single molecule analysis of RNA polymerase elongation reveals uniform kinetic behavior. *Proc Natl Acad Sci USA* 99(21):13538–13543.
34. Neuman KC, Abbondanzieri EA, Landick R, Gelles J, Block SM (2003) Ubiquitous transcriptional pausing is independent of RNA polymerase backtracking. *Cell* 115(4): 437–447.
35. Zamft B, Bintu L, Ishibashi T, Bustamante C (2012) Nascent RNA structure modulates the transcriptional dynamics of RNA polymerases. *Proc Natl Acad Sci USA* 109(23): 8948–8953.
36. Emsley P, Lohkamp B, Scott WG, Cowtan K (2010) Features and development of Coot. *Acta Crystallogr D Biol Crystallogr* 66(Pt 4):486–501.
37. Martinez-Rucobo FW, Sainsbury S, Cheung AC, Cramer P (2011) Architecture of the RNA polymerase-Spt4/5 complex and basis of universal transcription processivity. *EMBO J* 30(7):1302–1310.
38. Stroud J (2004) The Make-Na Server. Available at structure.usc.edu/make-na/server.html. Accessed June, 2016.
39. Barnes CO, et al. (2015) Crystal structure of a transcribing RNA polymerase II complex reveals a complete transcription bubble. *Mol Cell* 59(2):258–269.